Supplementary material: Evaluating the contribution of the unexplored photochemistry of aldehydes on the tropospheric levels of hydrogen.

Maria Paula Perez-Peña, Jenny A. Fisher, Dylan B. Millet, Hisashi Yashiro, Ray L. Langenfelds, Paul B. Krummel, Scott H. Kable

For a vertical profile comparison of the molecular hydrogen (H_2) we used the records from the Aircraft (AIA) flask sampling data from Krummel et al., 2021r measured over Tasmania. The seasonal average ratios of the H_2 measured at varying heights with respect to the ground values (from 1991 to 2000) were plotted against the average model estimates from 2015 and 2016 (see Figure S7). SON and DJF were the seasons for which GEOS-Chem represented best the evolution of H_2 with altitude. On the other hand, for MAM and JJA, the model was unable to capture the vertical gradient of the observations attributing more H_2 in height than the reported in the average nine year trend. This might be caused by enhanced modelled vertical transport of H_2.

References

Fu, T. M., Jacob, D. J., Wittrock, F., Burrows, J. P., Vrekoussis, M., & Henze, D. K. (2008). Global budgets of atmospheric glyoxal and methylglyoxal, and implications for formation of secondary organic aerosols. *Journal of Geophysical Research Atmospheres*, *113*(15). https://doi.org/10.1029/2007JD009505

Krummel, P. B., Langenfelds, R. L., & Loh, Z. (2021a). Atmospheric CO at Alert by Commonwealth Scientific and Industrial Research Organisation, dataset published as CO_ALT_surface-flask_CSIRO_data1 at WDCGG, ver. 2021-07-05-0440. https://doi.org/ttps://doi.org/10.50849/WDCGG{_}0016-4001-3001-01-02-9999

Krummel, P. B., Langenfelds, R. L., & Loh, Z. (2021b). Atmospheric CO at Cape Ferguson by Commonwealth Scientific and Industrial Research Organisation, dataset published as CO_CFA_surface-flask_CSIRO_data1 at WDCGG, ver. 2021-07-05-0440. https://doi.org/https://doi.org/10.50849/WDCGG{_}0016-5010-3001-01-02-9999

Krummel, P. B., Langenfelds, R. L., & Loh, Z. (2021c). Atmospheric CO at Cape Grim by Commonwealth Scientific and Industrial Research Organisation, dataset published as CO_CGO_surface-flask_CSIRO_data1 at WDCGG, ver. 2021-07-05-0440. https://doi.org/https://doi.org/10.50849/WDCGG{_}0016-5011-3001-01-02-9999

Krummel, P. B., Langenfelds, R. L., & Loh, Z. (2021d). Atmospheric CO at Casey by Commonwealth Scientific and Industrial Research Organisation, dataset published as CO_CYA_surface-flask_CSIRO_data1 at WDCGG, ver. 2021-07-05-0440. https://doi.org/https://doi.org/10.50849/WDCGG{_}0016-7004-3001-01-02-9999

Krummel, P. B., Langenfelds, R. L., & Loh, Z. (2021e). Atmospheric CO at Macquarie Island by Commonwealth Scientific and Industrial Research Organisation, dataset published as CO_MQA_surface-flask_CSIRO_data1 at WDCGG, ver. 2021-07-05-0440. https://doi.org/https://doi.org/10.50849/WDCGG{_}0016-5015-3001-01-02-9999

Krummel, P. B., Langenfelds, R. L., & Loh, Z. (2021f). Atmospheric CO at Mauna Loa by Commonwealth Scientific and Industrial Research Organisation, dataset published as CO_MLO_surface-flask_CSIRO_data1 at WDCGG, ver. 2021-07-05-0440. https://doi.org/https://doi.org/10.50849/WDCGG{_}0016-5002-3001-01-02-9999

Krummel, P. B., Langenfelds, R. L., & Loh, Z. (2021g). Atmospheric CO at Mawson by Commonwealth Scientific and Industrial Research Organisation, dataset published as CO_MAA_surface-flask_CSIRO_data1 at WDCGG, ver. 2021-07-05-0440. https://doi.org/https://doi.org/10.50849/WDCGG{_}0016-7005-3001-01-02-9999

Krummel, P. B., Langenfelds, R. L., & Loh, Z. (2021h). Atmospheric CO at South Pole by Commonwealth Scientific and Industrial Research Organisation, dataset published as CO_SPO_surface-flask_CSIRO_data1 at WDCGG, ver. 2021-07-05-0440. https://doi.org/https://doi.org/10.50849/WDCGG{_}0016-7011-3001-01-02-9999

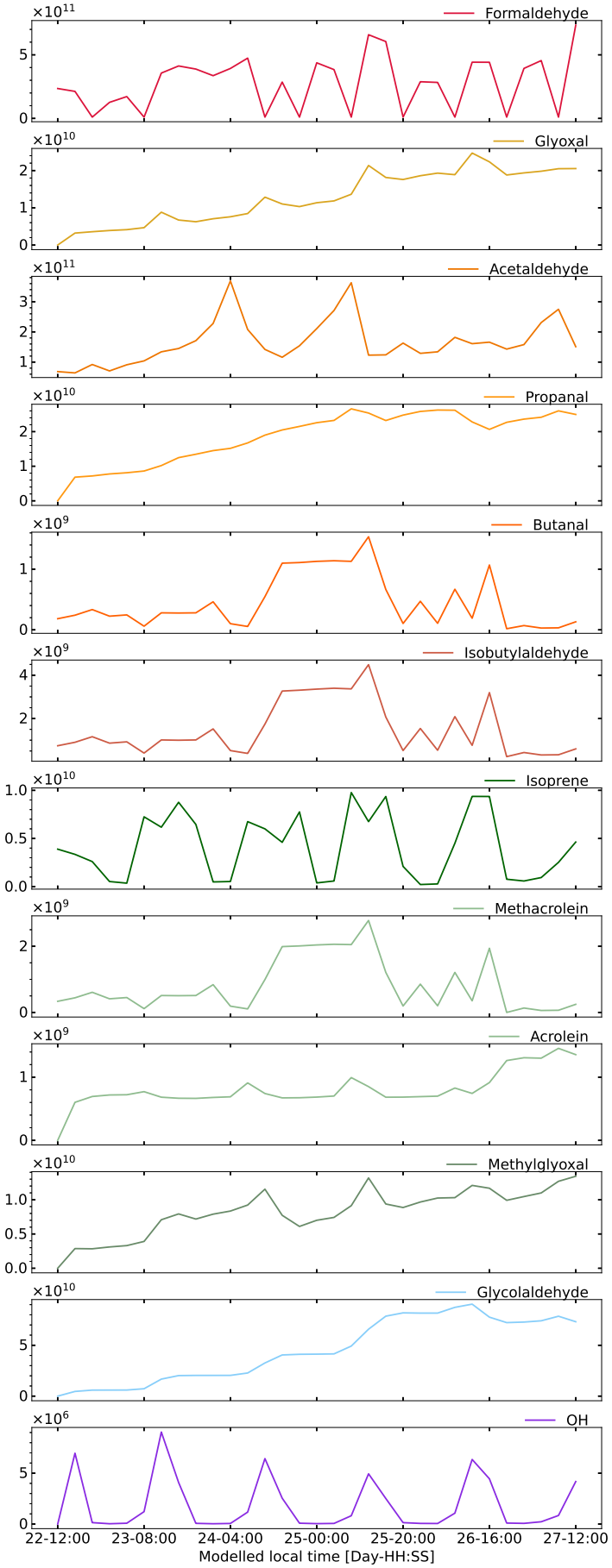

Figure S1: Time series for selected modelled species in molecules cm^{-3} from the baseline box model simulation in London starting at noon on the 22^{nd} of July 2012.

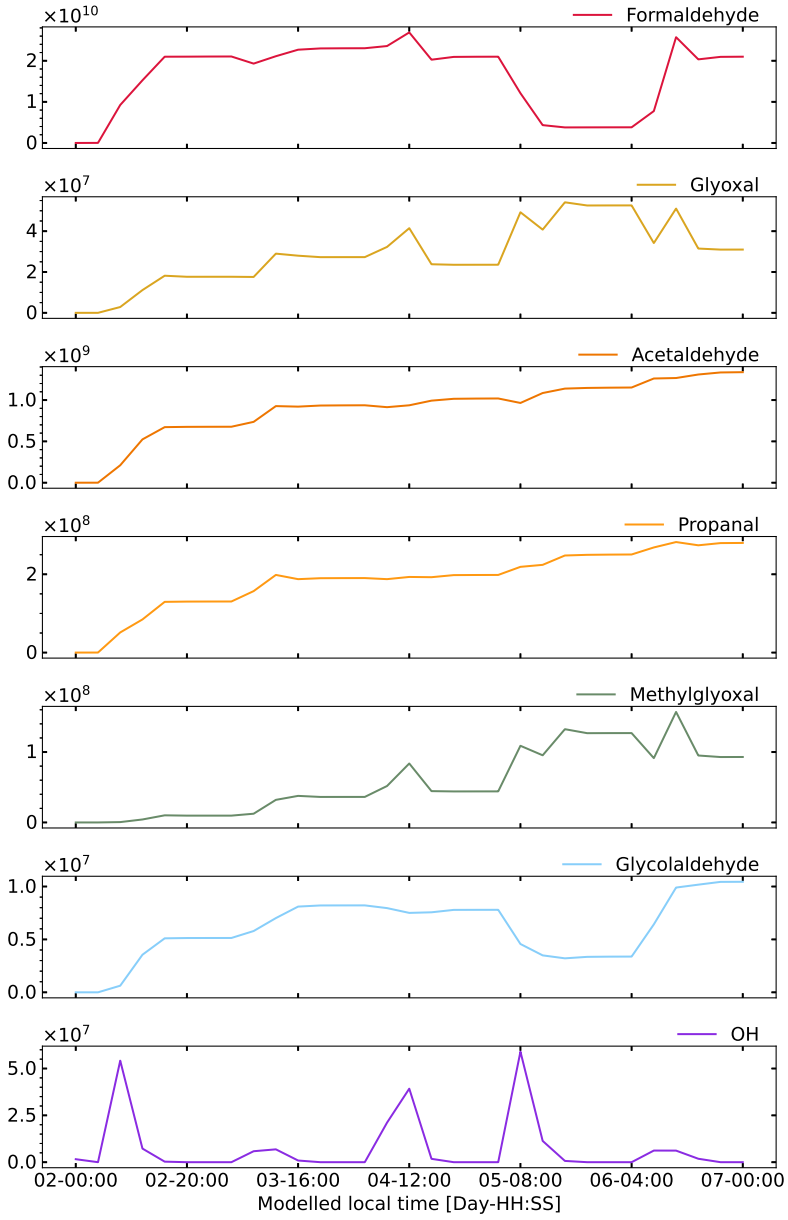

Figure S2: Time series for selected modelled species in molecules cm^{-3} from the baseline box model simulation in Cape Verde starting at midnight on the 2^{nd} of January 2015.

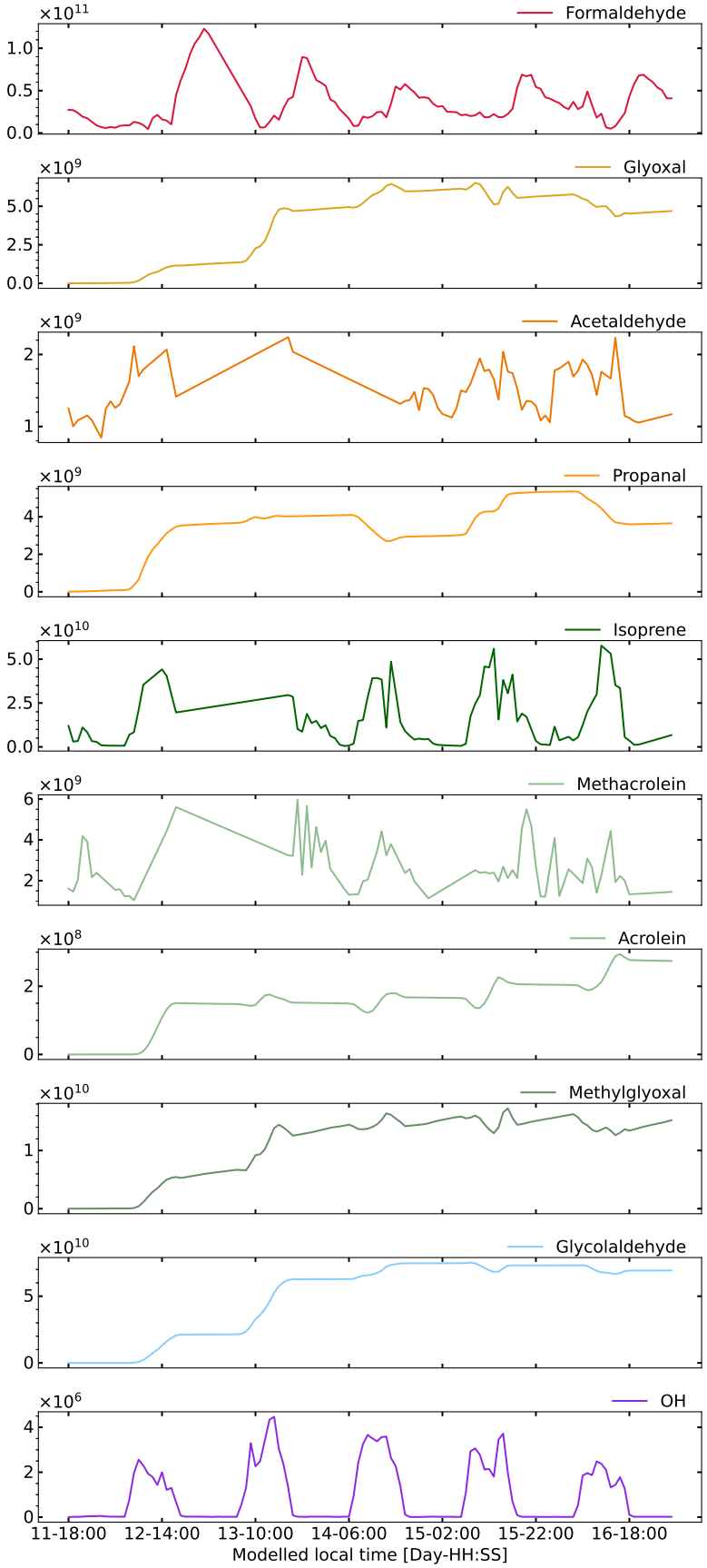

Figure S3: Time series for selected modelled species in molecules cm^{-3} from the baseline box model simulation in Borneo starting at 18:00 on the 11^{th} of July 2008.

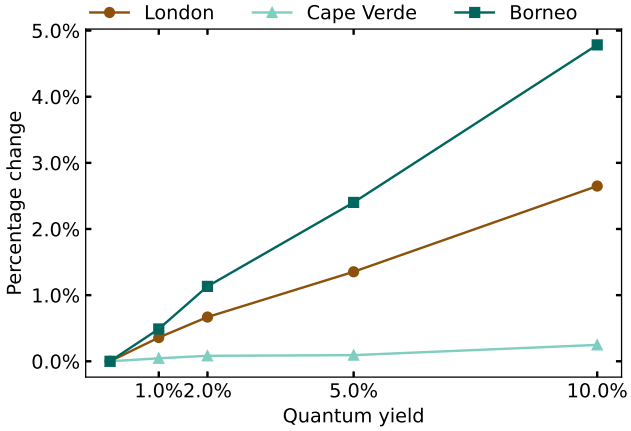

Figure S4: Percentage change in the total rate of production of H_2 from aldehydes for varying quantum yields calculated relative to the baseline simulation at the three tested sites for 1 modelled day (local time)

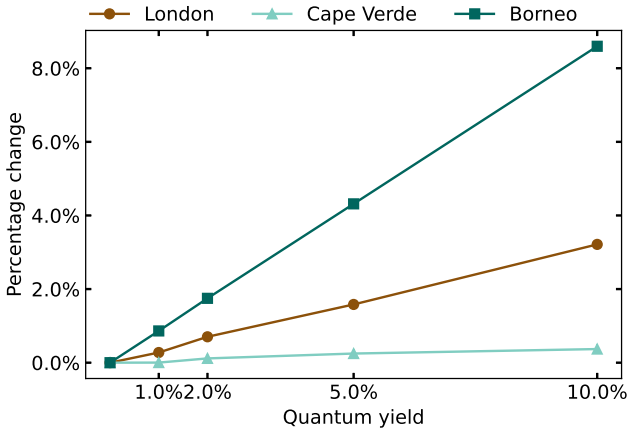

Figure S5: Percentage change in the total rate of production of H_2 from aldehydes for varying quantum yields at the three tested sites for 5 modelled days (local time)

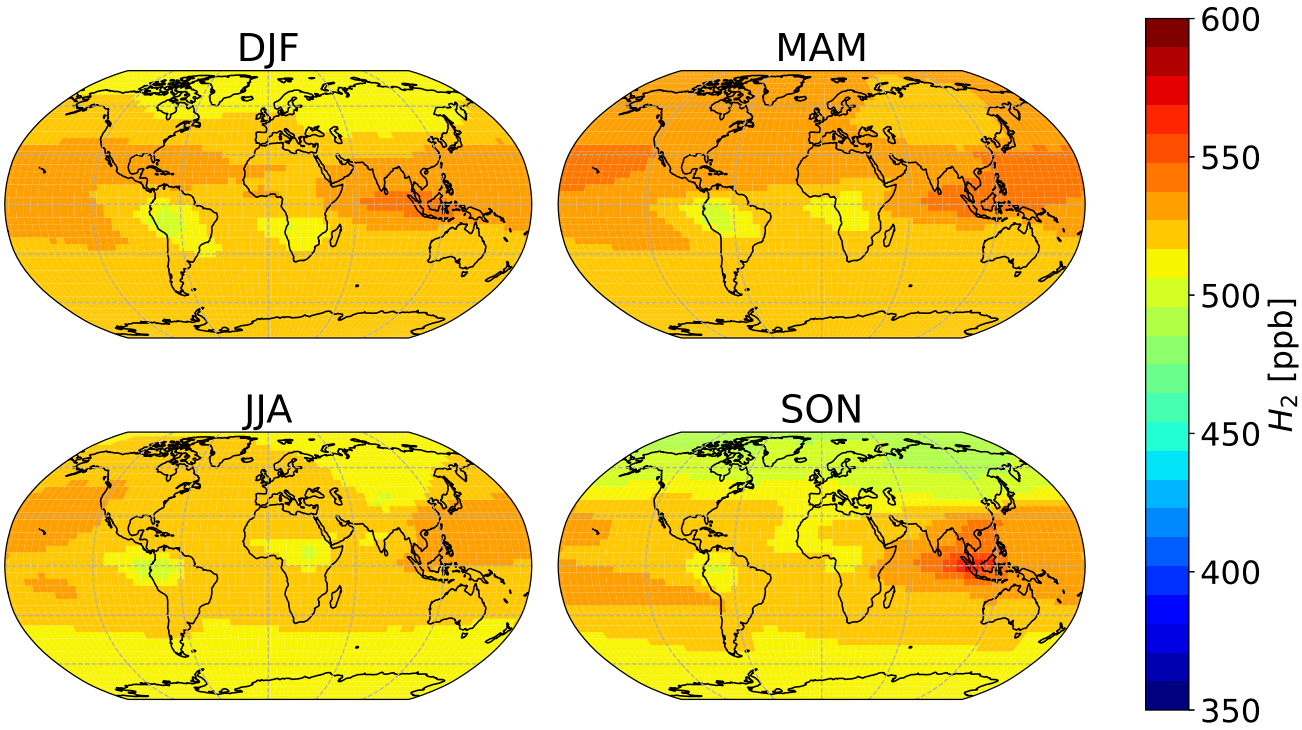

Figure S6: Average modelled mixing rations of H_2 per season estimated with GEOS-Chem at 500 hPa for 2015 and 2016.

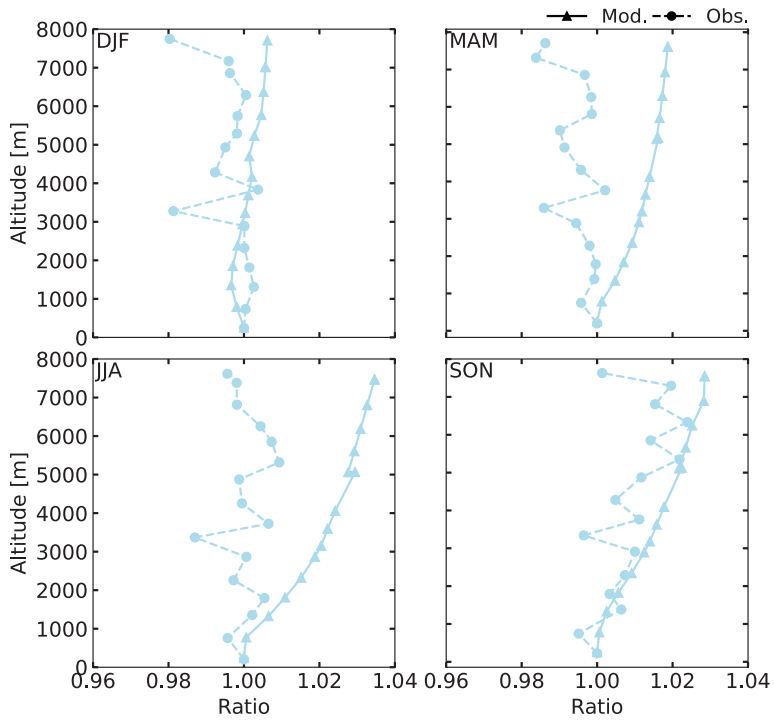

Figure S7: Seasonal comparison between average modelled (triangles) and average observed (circles) H_2 estimated ratios at different heights with respect to the surface layer. Modelled averaged values are from 2015 and 2016. Observations averaged values are those from the Aircraft (AIA) flask sampling data from Krummel et al., 2021r

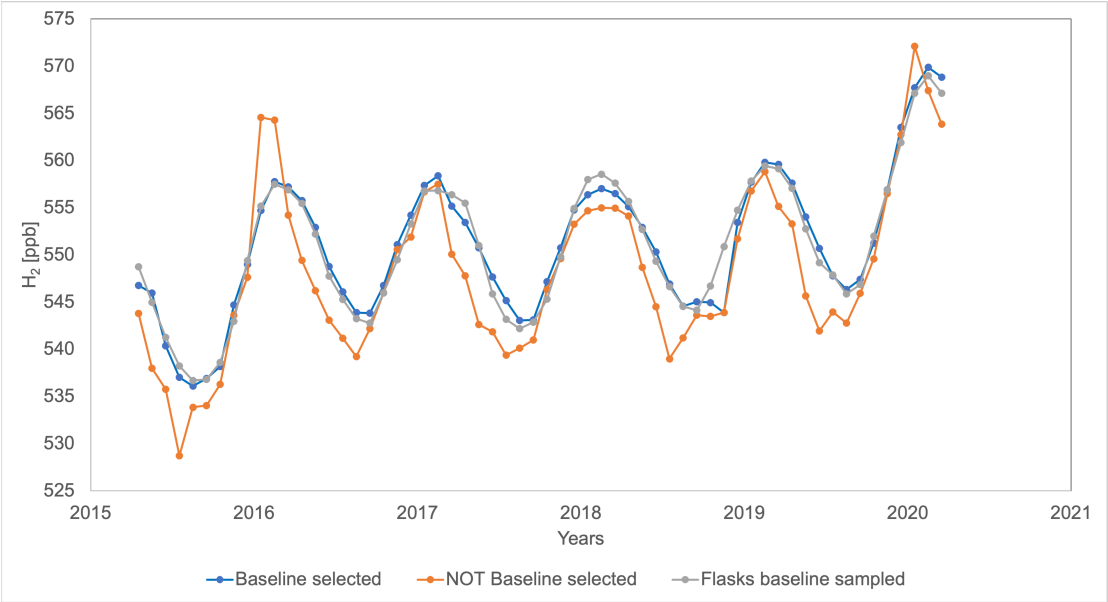

Figure S8: Comparison between baseline-selected in-situ data, baseline-sampled data measured with a PDD detector (blue and orange line) and flask baseline sampled by CSIRO at Cape Grim from April 2015.

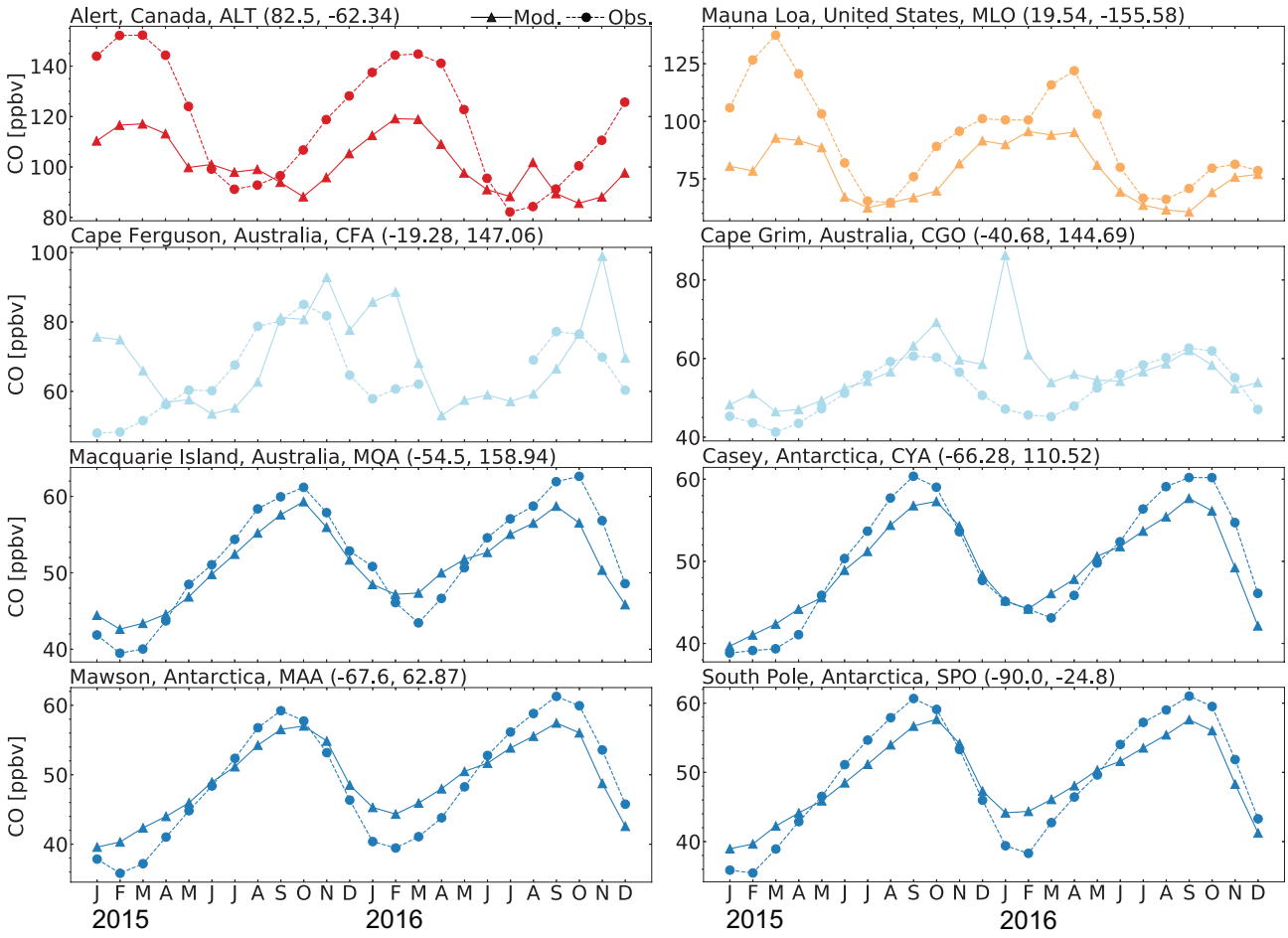

Figure S9: Seasonal cycle comparisons of CO at five sites from the CSIRO dataset (Krummel et al., 2021a, 2021b, 2021c, 2021d, 2021e, 2021f, 2021g, 2021h, 2021i) reported Flask Data for 2015 and 2016, the dash line with circle markers corresponds to observed values and the continuous line with triangle markers corresponds to modelled values in GEOS-Chem.

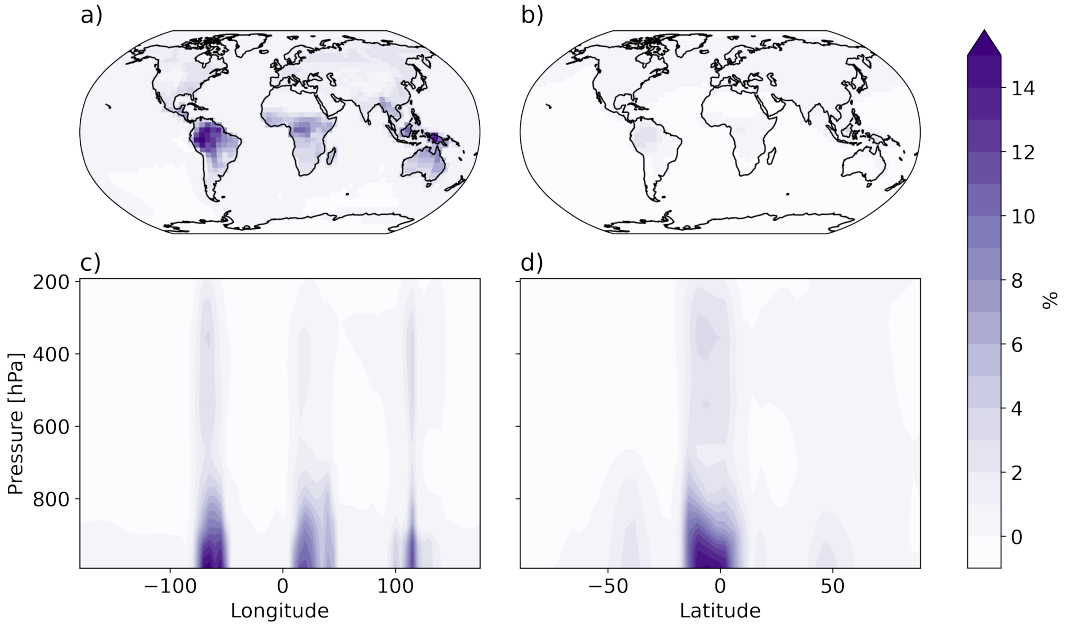

Figure S10: Percentage difference on the chemical production of H_2 between the 1% production of H_2 scenario and the baseline for a year a) At the surface level, b) At 500 hPa, c) Longitude section at 2 N and d) Latitude section at -70 W

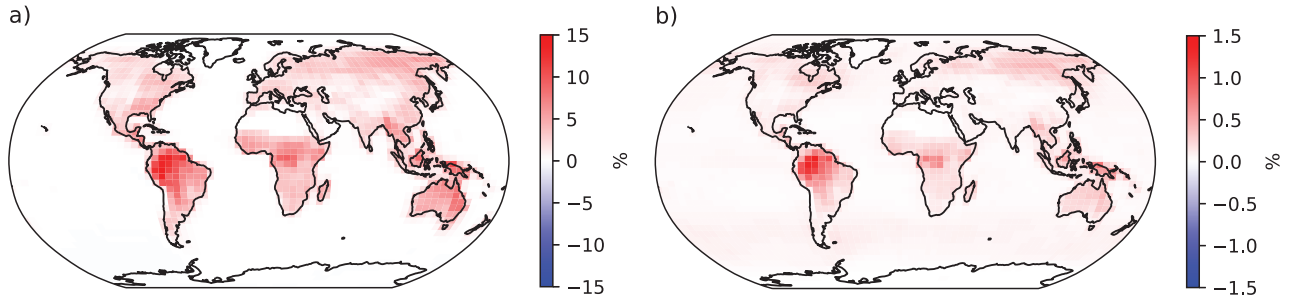

Figure S11: Percentage difference on the chemical production of H_2 between the 1% production of H_2 scenario and the baseline for a year at the surface layer from the photolysis of a) methylglyoxal b) acetaldehyde, HPALD, glycolaldehyde, methacrolein, lumped aldehydes with more than 3 carbon atoms RCHO (integrated)

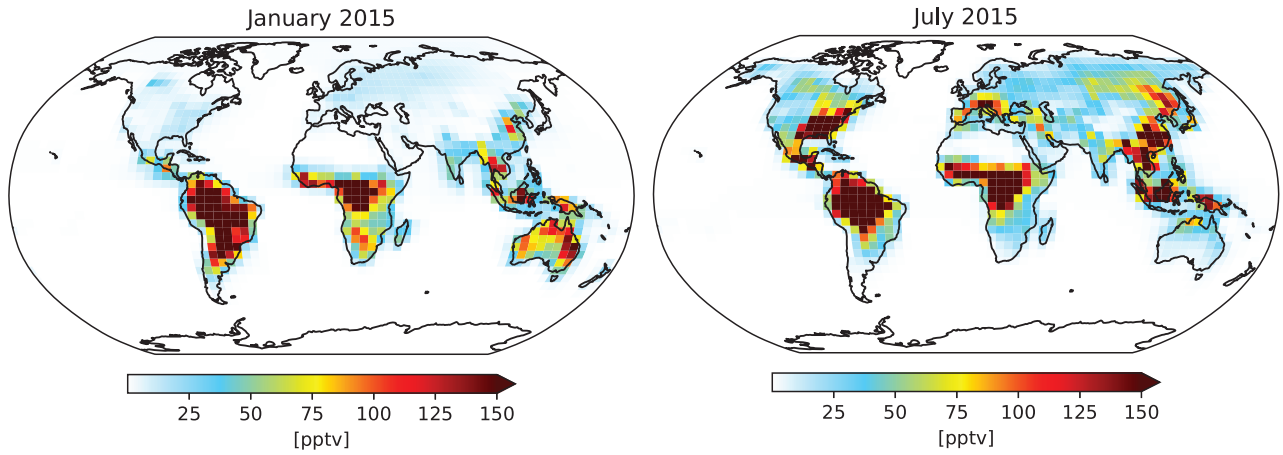

Figure S12: Simulated mixing ratios of methylglyoxal at the surface layer for January and July 2015. The modelled magnitudes of methylglyoxal in our GEOS-Chem simulation are comparable to those shown by Fu et al., 2008 in their Figure 2b.

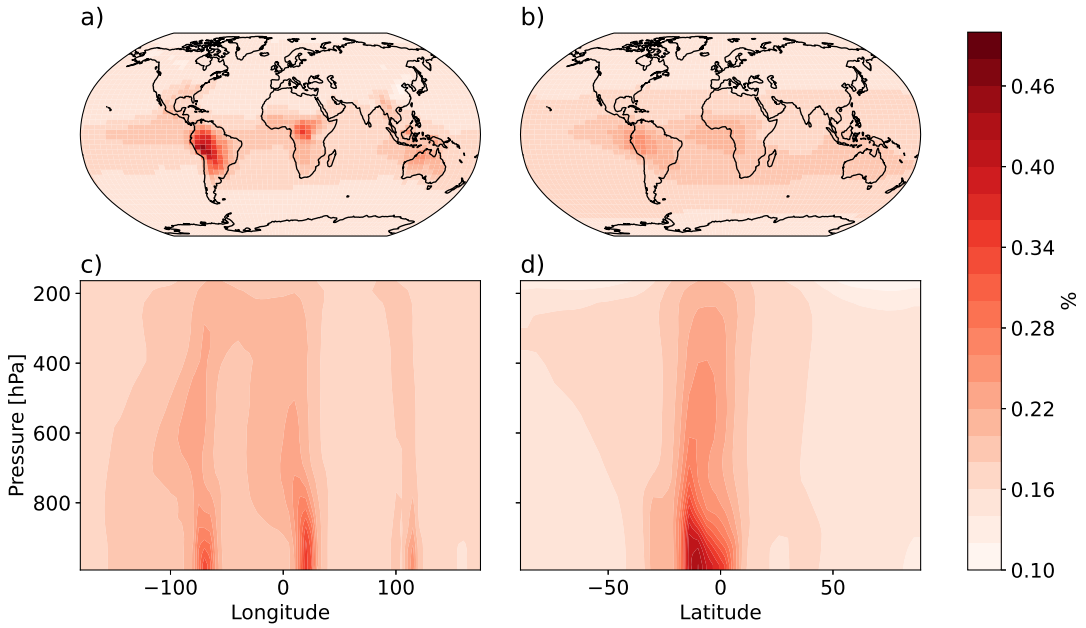

Figure S13: Percentage difference on the modelled mixing ratios of H_2 between the 1% production of H_2 scenario and the baseline for a year a) At the surface level, b) At 500 hPa, c) Longitude section at 2deg N and d) Latitude section at -70deg W

Krummel, P. B., Langenfelds, R. L., & Loh, Z. (2021i). Atmospheric CO by Aircraft (over Bass Strait and Cape Grim), Commonwealth Scientific and Industrial Research Organisation, dataset published as CO_AIA_aircraft-flask_CSIRO_data1 at WDCGG, ver. 2021-07-05-0440. https://doi.org/https://doi.org/10.50849/WDCGG{_}0016-8003-3001-05-02-9999{\}

Krummel, P. B., Langenfelds, R. L., & Loh, Z. (2021j). Atmospheric H2 at Alert by Commonwealth Scientific and Industrial Research Organisation, dataset published as H2_ALT_surface-flask_CSIRO_data1 at WDCGG, ver. 2021-07-05-0440. https://doi.org/https://doi.org/10.50849/WDCGG{_}0016-4001-4001-01-02-9999

Krummel, P. B., Langenfelds, R. L., & Loh, Z. (2021k). Atmospheric H2 at Cape Ferguson by Commonwealth Scientific and Industrial Research Organisation, dataset published as H2_CFA_surface-flask_CSIRO_data1 at WDCGG, ver. 2021-07-05-0440. https://doi.org/https://doi.org/10.50849/WDCGG{_}0016-5010-4001-01-02-9999

Krummel, P. B., Langenfelds, R. L., & Loh, Z. (2021l). Atmospheric H2 at Cape Grim by Commonwealth Scientific and Industrial Research Organisation, dataset published as H2_CGO_surface-flask_CSIRO_data1 at WDCGG, ver. 2021-07-05-0440. https://doi.org/https://doi.org/10.50849/WDCGG{_}0016-5011-4001-01-02-9999

Krummel, P. B., Langenfelds, R. L., & Loh, Z. (2021m). Atmospheric H2 at Casey by Commonwealth Scientific and Industrial Research Organisation, dataset published as H2_CYA_surface-flask_CSIRO_data1 at WDCGG, ver. 2021-07-05-0440. https://doi.org/https://doi.org/10.50849/WDCGG{_}0016-7004-4001-01-02-9999

Krummel, P. B., Langenfelds, R. L., & Loh, Z. (2021n). Atmospheric H2 at Macquarie Island by Commonwealth Scientific and Industrial Research Organisation, dataset published as H2_MQA_surface-flask_CSIRO_data1 at WDCGG, ver. 2021-07-05-0440. https://doi.org/https://doi.org/10.50849/WDCGG{_}0016-5015-4001-01-02-9999

Krummel, P. B., Langenfelds, R. L., & Loh, Z. (2021o). Atmospheric H2 at Mauna Loa by Commonwealth Scientific and Industrial Research Organisation, dataset published as H2_MLO_surface-flask_CSIRO_data1 at WDCGG, ver. 2021-07-05-0440. https://doi.org/https://doi.org/10.50849/WDCGG{_}0016-5002-4001-01-02-9999,

Krummel, P. B., Langenfelds, R. L., & Loh, Z. (2021p). Atmospheric H2 at Mawson by Commonwealth Scientific and Industrial Research Organisation, dataset published as H2_MAA_surface-flask_CSIRO_data1 at WDCGG, ver. 2021-07-05-0440. https://doi.org/https://doi.org/10.50849/WDCGG{_}0016-7005-4001-01-02-9999

Krummel, P. B., Langenfelds, R. L., & Loh, Z. (2021q). Atmospheric H2 at South Pole by Commonwealth Scientific and Industrial Research Organisation, dataset published as H2_SPO_surface-flask_CSIRO_data1

at WDCGG, ver. 2021-07-05-0440. https://doi.org/https://doi.org/10.50849/WDCGG{_}0016-7011-4001-01-02-9999

Krummel, P. B., Langenfelds, R. L., & Loh, Z. (2021r). Atmospheric H2 by Aircraft (over Bass Strait and Cape Grim), Commonwealth Scientific and Industrial Research Organisation, dataset published as H2_AIA_aircraft-flask_CSIRO_data1 at WDCGG, ver. 2021-07-05-0440. https://doi.org/https://doi.org/10.50849/WDCGG{_}0016-8003-4001-05-02-9999

Table S1: List of aldehydes in the MCM, along with photolysis products and rates (J [s^{-1}]) for the H_2 channel estimated with 1%, 2%, 5% and 10% quantum yields applied across wavelengths.

Aldehyde	**MCM ID**	**Photolysis products**[a]	**JID**	**J 1% qy**	**J 2% qy**	**J 5% qy**	**J 10% qy**
Formaldehyde	HCHO[b]	H2 + CO	J12	-	-	-	-
Glyoxal	GLYOX[b]	CO + CO + H2	J31	-	-	-	-
Acetaldehyde	CH3CHO	CH2CO[c] + H2	J62	4.37E-07	8.74E-07	2.18E-06	4.37E-06
Propanal	C2H5CHO	C2H4 + H2 + CO	J63	5.68E-07	1.14E-06	2.84E-06	5.68E-06
Butanal	C3H7CHO	C3H6 + H2 + CO	J64	6.76E-07	1.35E-06	3.38E-06	6.76E-06
Isobutylaldehyde	IPRCHO	C3H6 + H2 + CO	J65	5.49E-07	1.10E-06	2.74E-06	5.49E-06
Acrolein	ACR	C2H2 + H2 + CO	J66	2.44E-06	4.89E-06	1.22E-05	2.44E-05
Methacrolein	MACR	C3H4 + H2 + CO	J67	3.05E-07	6.09E-07	1.52E-06	3.05E-06
Methylglyoxal	MGLYOX	CH2CO[c] + H2 + CO	J68	4.42E-07	8.83E-07	2.21E-06	4.42E-06
HPALD	HCOCH2OOH	H2 + Other products	J69	4.65E-08	9.30E-08	2.32E-07	4.65E-07
Glycolaldehyde	HOCH2CHO	HCHO + H2 + CO	J70	1.07E-07	2.15E-07	5.37E-07	1.07E-06
3-Hydroxy 2-Methylpropanal	HOIPRCHO	H2 + Other products	J71[d]	6.76E-07	1.10E-06	3.38E-06	6.76E-06
Lactaldehyde	CH3CHOHCHO	H2 + Other products	J71[d]	6.76E-07	1.10E-06	3.38E-06	6.76E-06
3-Oxopentanal	CO3C4CHO	H2 + Other products	J71[d]	6.76E-07	1.10E-06	3.38E-06	6.76E-06
3-Hydroxy-pentanal	HO3C4CHO	H2 + Other products	J71[d]	6.76E-07	1.10E-06	3.38E-06	6.76E-06
3-Hydroxypropanal	HOC2H4CHO	H2 + Other products	J71[d]	6.76E-07	1.10E-06	3.38E-06	6.76E-06
2-Hydroxybutanal	HO3C3CHO	H2 + Other products	J71[d]	6.76E-07	1.10E-06	3.38E-06	6.76E-06
4-Hydroxybutanal	HOC3H6CHO	H2 + Other products	J71[d]	6.76E-07	1.10E-06	3.38E-06	6.76E-06

[a] Expressed with the identification used in the MCM.

[b] Species in MCM that already include the photolytic generation of H_2. The photolysis rates were kept the same for all tests.

[c] The ketene CH_2CO generated in the photolysis channel was replaced with glycolaldehyde as described in the text.

[d] In absence of aldehyde-specific cross section measurements, the photolysis rate of butanal was used as a surrogate in each case.

Table S2: Calculated metrics at each measuring site from the Krummel et al., 2021j, 2021k, 2021l, 2021m, 2021n, 2021o, 2021p, 2021q dataset

Site ID	Site name	Lat	Lon	Hemisphere	Lat. band	Gas	Start[a]	End[b]	N. obs[c]	Mean Mod. [ppb]	Mean Obs. [ppb]	r	RMSE	MB	NMB	MFB	NME	FE	FB
ALT	Alert	82.4991	-62.3415	NH	HNH	H_2	2015-01	2016-12	24	499.91	489.93	0.92	12.97	9.98	2.04	0.02	2.20	2.19	2.02
MLO	Mauna Loa	19.5362	-155.5762	NH	LNH	H_2	2015-01	2016-12	24	533.35	536.51	0.56	9.59	-3.16	-0.59	-0.01	1.25	1.27	-0.60
CFA	Cape Ferguson	-19.2773	147.0584	SH	LSH	H_2	2015-01	2016-12	20	486.22	546.30	0.70	60.64	-60.08	-11.00	-0.12	11.00	11.66	-11.66
CGO	Cape Grim	-40.6822	144.6883	SH	LSH	H_2	2015-01	2016-12	24	509.00	547.37	0.77	38.79	-38.37	-7.01	-0.07	7.01	7.27	-7.27
MQA	Macquarie Island	-54.4985	158.9385	SH	HSH	H_2	2015-01	2016-12	24	514.49	547.78	0.88	33.43	-33.29	-6.08	-0.06	6.08	6.27	-6.27
CYA	Casey	-66.2833	110.5167	SH	HSH	H_2	2015-01	2016-12	24	516.65	546.93	0.92	30.39	-30.28	-5.54	-0.06	5.54	5.69	-5.69
MAA	Mawson	-67.6047	62.8706	SH	HSH	H_2	2015-01	2016-12	14	518.69	551.72	0.81	33.16	-33.03	-5.99	-0.06	5.99	6.17	-6.17
SPO	South Pole	-89.9969	-24.8	SH	HSH	H_2	2015-01	2016-12	24	516.67	547.13	0.92	30.57	-30.47	-5.57	-0.06	5.57	5.73	-5.73

[a]Corresponds to the first date available in the measurements from Krummel et al., (2021a-i) used in the calculation of metrics.

[b]Corresponds to the last date available in the measurements from Krummel et al., (2021a-i) used in the calculation of metrics.

[c]Number of measurements used to compare during the period covered by the start [a] and end [b] dates.